JOURNAL OF MATERIALS SCIENCE 32 (1997) 809–814

High temperature flow and failure processes in an Al–13 wt % Si eutectic alloy

R. K. MAHIDHARA
Tessera Inc., 3099 Orchard Drive, San Jose, CA 95134, USA

A. K. MUKHERJEE
Department of Chemical Engineering and Materials Science, University of California, Davis, CA 95616, USA

A maximum elongation of 250% was achieved in a Al–13 wt % Si eutectic alloy (~ 18 μm grain size) when deformation was carried out at 557 °C at a strain rate of $1 \times 10^{-2}\,s^{-1}$. The shapes of the true stress–true strain curves obtained in this investigation are different from those reported by Chung and Cahoon [1]. It is felt that this is due to differences in the processing of the alloys used in the two investigations. The higher elongation obtained at a strain-rate of $1 \times 10^{-2}\,s^{-1}$ as compared to $4.6 \times 10^{-4}\,s^{-1}$ is attributed to a higher strain rate sensitivity, lower rain and particle coarsening and a lower level of cavitation at the former strain rate. It is believed that the mechanism of high temperature flow in this system is by grain boundary sliding accommodated by dislocation motion. The latter is rate controlled by the climb of dislocations over hard Si particles.

1. Introduction

Superplastic deformation is characterized by a high strain rate sensitivity of the flow stress and usually occurs above half the absolute melting temperature [2]. High elongations are obtained in superplastic alloys at very low flow stresses and the work hardening exponent is quite small. The ductility peak, however, lies within a narrow range of temperatures and strain rates and this phenomenon is generally observed in extremely fine grained alloys (usually below 10 μm).

Initially a number of superplastic alloys were developed in which two phases were present in approximately equal proportions. These alloys were of nearly eutectic or eutectoid composition and did not, in general, possess commercially attractive mechanical properties. It was later found that, if a fine grain size could be rendered stable at the initial level during deformation (e.g., by the introduction of small amounts of extremely fine, dispersed second phase particles), even single phase alloys could be deformed superplastically [3].

Previous work on Al–13 wt % Si showed low superplastic ductility despite high values for strain-rate sensitivity [1]. Microstructural observations indicated that the silicon particles grow by a factor of 2–3 during deformation. This, along with grain growth, cause hardening of the matrix and also the formation of cavities at the particle/matrix interface.

This study was initiated to evaluate both the mechanical and microstructural aspects of high temperature flow and failure in an Al–13 wt % Si alloy obtained in sheet form.

2. Experimental procedure

The Al–13 wt % Si alloy used in the present work was obtained from Kaiser Aluminium and Chemical Company of Pleasanton, CA, USA in the form of a 3.2 mm thick sheet. The alloy had an initial grain-size (measured using the random intercept length technique) of ~ 18 μm whilst the silicon particle size (measured using Johnson–Saltykov analysis [4]) was ~ 1.5 μm.

Tensile tests were carried out on 3.2 mm thick strip specimens of 7 mm gauge length and 6.34 mm width (cut parallel to the rolling direction) on an MTS automated machine in an argon atmosphere. Tensile tests involved both differential strain-rate testing as well as uniaxial testing. Elevated temperatures were achieved using a Quad elliptical furnace controlled to within ± 5 °C. Metallographic investigations using optical, scanning and transmission electron microscopes were performed. The grain boundaries and silicon particles were revealed by alternately etching with Keller's reagent and removing the excess etchant using 1 μm diamond paste. Johnson–Saltykov analysis was performed on the silicon particles by assuming that the particles were spherical in shape. A Phillips EM400 microscope operated at 100 kV was used to obtain information on the internal structure. Thin foils for the transmission electron microscope (TEM) work were prepared by electropolishing 3 mm discs at -60 °C in 25% nitric acid–75% methanol solution at 20 mV.

0022–2461

3. Results

The true stress–true strain curves obtained at a test temperature of 557 °C are shown in Fig. 1. As can be seen from this figure, there is a significant decrease in the strain to failure with decreasing strain rate. This decrease in ductility is believed to be due to the drop in the strain rate sensitivity, m ($\delta \ln \sigma / \delta \ln \dot{\varepsilon}$) where σ is the stress and $\dot{\varepsilon}$ the strain rate, with decreasing strain rate. This effect is shown in Fig. 2 for tests carried out at three different temperatures. From this figure, it is seen that m decreases not only with a decrease in the strain rate, in contrast to an earlier report [1] but also with a lowering of the test temperature. The fact that the m value is low suggests that, this alloy is not extensively superplastic. In addition, it has been observed that the value of m does not decrease from a value of 0.22 at a strain-rate greater than $10^{-3}\,s^{-1}$ but increases to 0.26 at $10^{-2}\,s^{-1}$, which again suggests that the material is not truely representative of a superplastic material. Fig. 3 shows the flow stress of the alloy as a function of strain rate for three different test temperatures. A sigmoidal shape, characteristic of high temperature deformation, is immediately obvious, particularly at the lowest and highest test temperatures.

There is a significant difference in the shapes of the true stress–true strain curves obtained in our investigation and the work of Chung and Cahoon [1]. In particular, while the earlier work reported a kind of sinosoidal σ–ε curves due to strain softening and strain hardening in the alloy at strain rates equal to or less than $4.6 \times 10^{-3}\,s^{-1}$ beyond maximum true stress [1], only strain softening was observed in the present investigation. Strain softening is merely a reflection of the fall in load carrying capacity of the minimum cross-section of the extended test piece, in addition to microstructural effects. It is believed that the clue to these differences in behaviour lies in the differences in the processing history of the alloys used in the two investigations. The alloy examined in the earlier study [1], was hot-rolled at 793 K to a thickness of 2.5 mm which, reduced the cross-sectional areas by more than 300%, and then annealed for 2 h at the same temperature as a final treatment. The structure of present alloy has not been structurally modified prior to thermomechanical processing. However it has received a more severe thermomechanical treatment since the silicon particles in the as-received alloy are much finer ($\sim$1.5 μm) in the as-received condition as against $\sim$5 μm in the earlier alloy which was initially modified with 0.1% NaCl prior to thermomechanical processing [3]. In addition, at 557 °C, whereas the average particle in our alloy after failure is $\sim$4 μm, at a constant strain rate of $10^{-2}\,s^{-1}$ ($\sim$250%), the corresponding value after $\sim$310% failure elongation at an initial strain rate of $1.85 \times 10^{-2}\,s^{-1}$ was assessed as $\sim$8 μm [1].

Quantitative metallography was performed in the present investigation to understand the role of particle and grain coarsening in the deformation behaviour of the alloy. The coarsening behaviour of the silicon

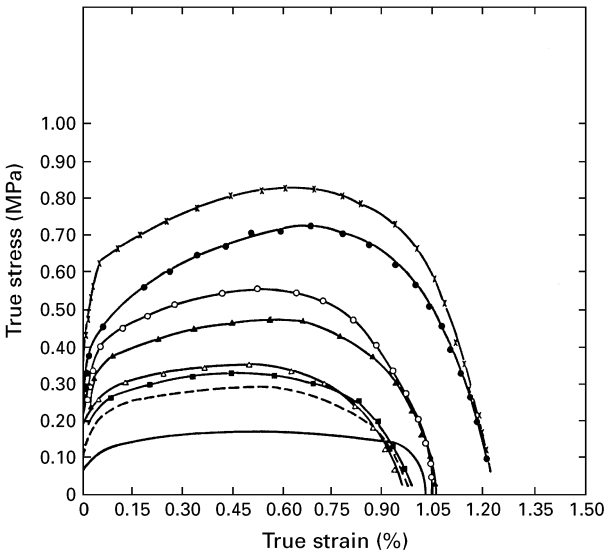

Figure 1 True stress–true strain curves for Al–13 wt % Si at a test temperature of 557 °C and at strain-rates of (×) 1×10^{-2}, (●) 5×10^{-3}, (○) 1×10^{-3}, (▲) 5×10^{-4}, (△) 2×10^{-4}, (■) 1×10^{-4}, (– –) 5×10^{-5}, (—) 1×10^{-5}.

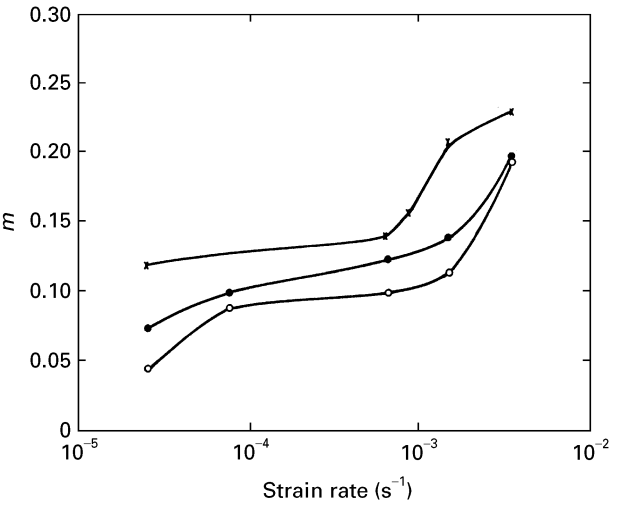

Figure 2 Plot of strain-rate sensitivity parameter, m, versus strain-rate computed from Fig. 1. Data were measured at temperatures of; (○) 477 °C, (●) 517 °C and (×) 557 °C.

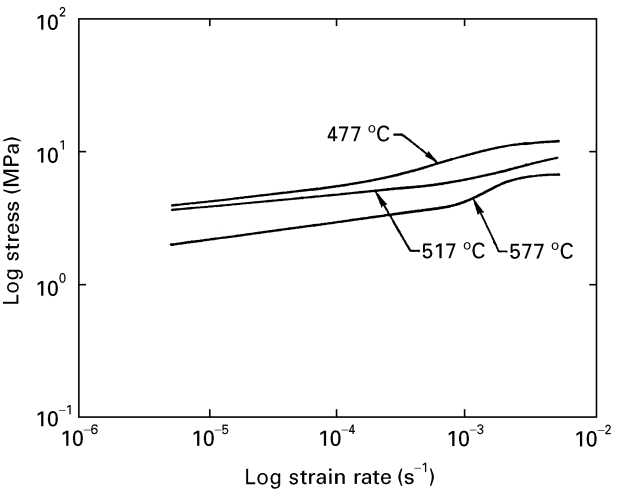

Figure 3 Log (stress) versus log (strain-rate) at three different temperatures.

particles as a function of annealing time at 560 °C (in the absence of an applied stress) is shown in Fig. 4. Fig. 5 shows the corresponding grain growth behaviour. It should be noted from these two figures that on annealing for 4 h, the silicon particles coarsen by a factor of 3 while the grains coarsen by a factor of 2. The application of a load, however, enhances the rate of grain growth, while the particle coarsening rate is not significantly altered. This was evident upon comparing both the particle and grain sizes before and after testing a sample to fracture at 557 °C at a strain rate of $1 \times 10^{-2}\ s^{-1}$. In this case both the silicon particles and the grains grew by a factor of 3. This suggests that, at least at slow strain rates, enhanced grain growth and particle coarsening would lead to a low strain rate sensitivity (m) and a high level of cavitation [1]. With a decrease in strain rate, the coarsening of both would be enhanced leading to an increase in the cavitation level and thus a decrease in the ductility to failure.

In this investigation, cavities were observed at strain-rates less than $5 \times 10^{-4}\ s^{-1}$; however, only at true strain levels greater than 0.7. Few or no cavities were observed at strain-rates equal to or greater than $5 \times 10^{-3}\ s^{-1}$. Fig. 6 shows optical micrographs of

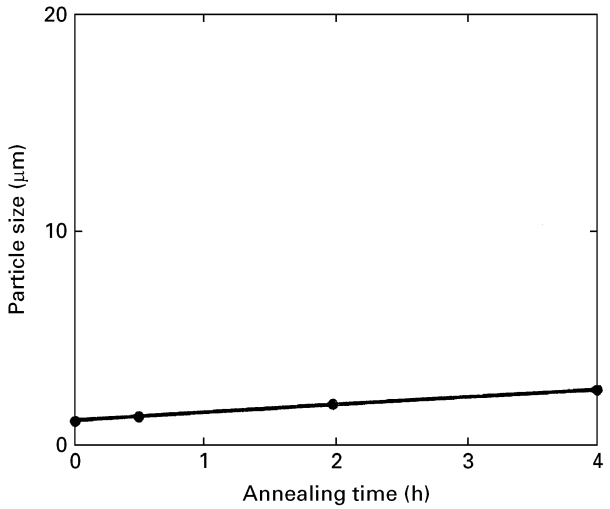

Figure 4 Plot of particle size versus annealing time at 560 °C determined using Johnson–Saltykov analysis.

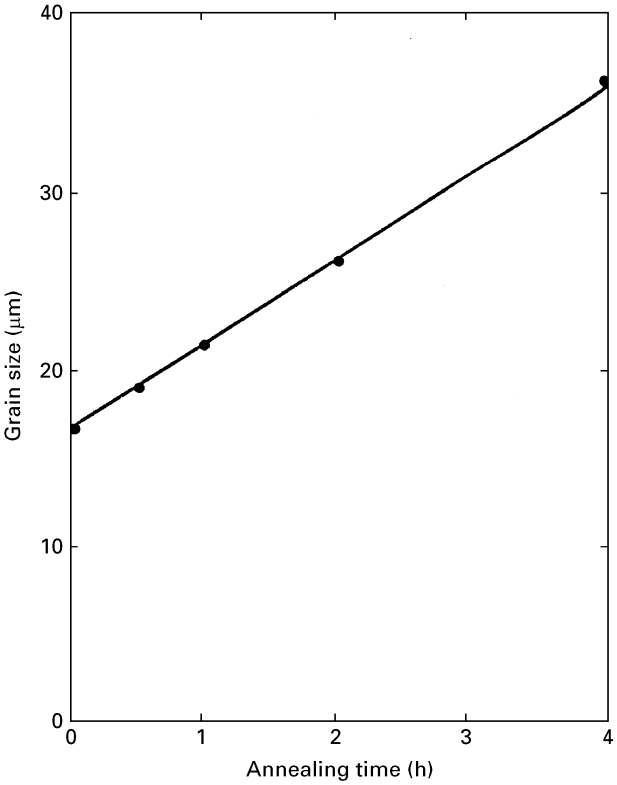

Figure 5 Plot of grain-size (determined using random intercept length technique) versus annealing time at a temperature of 560 °C.

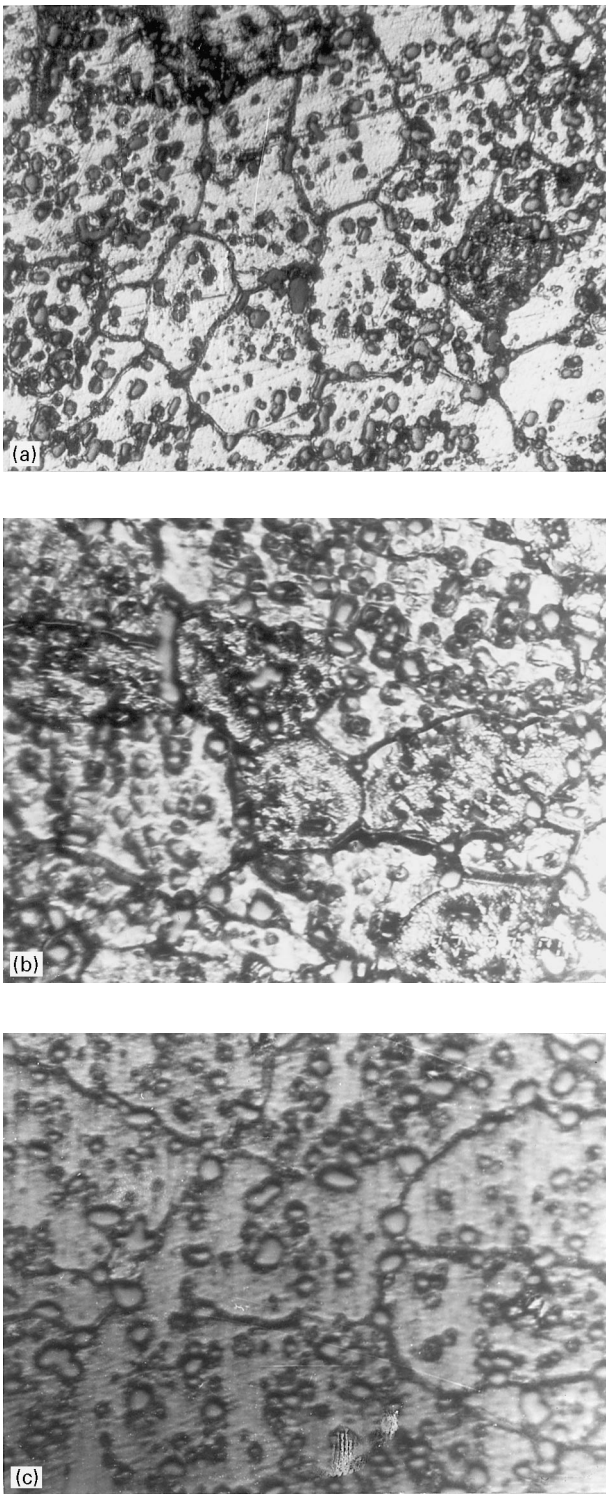

Figure 6 Optical micrographs of the Al–13 wt % Si alloy (a) as-received condition; taken after deformation at a temperature of 557 °C and at a strain-rate of $1 \times 10^{-2}\ s^{-1}$ to (b) $\varepsilon = 0.69$ (100%) and (c) $\varepsilon_{FAILURE} = 1.25$ (250%), (d) cavities in failed specimen in association with hard Si particles.

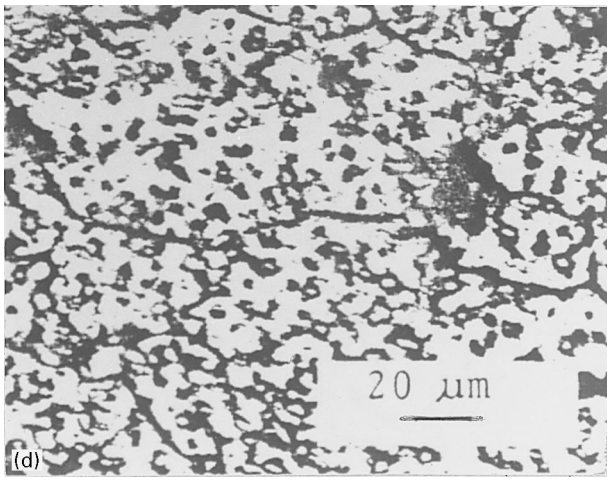

Figure 6 Continued.

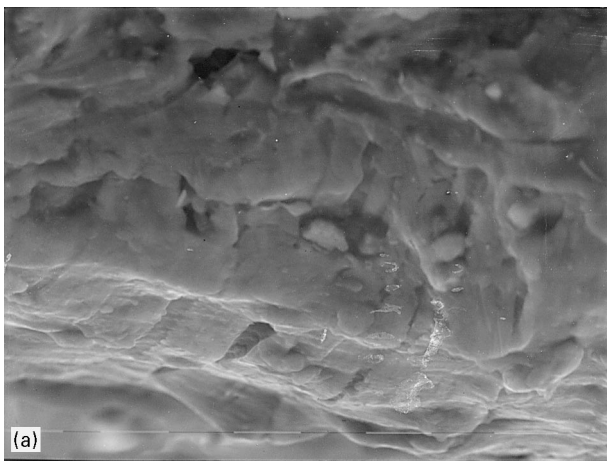

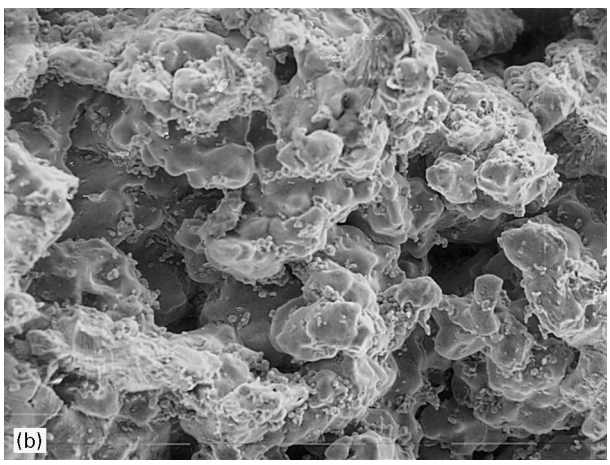

Figure 7 Scanning electron fractographs of the Al–13 wt % Si taken after deforming at a temperature of 557 °C and at strain-rates of (a) $1 \times 10^{-2}\ s^{-1}$ and (b) $1 \times 10^{-5}\ s^{-1}$.

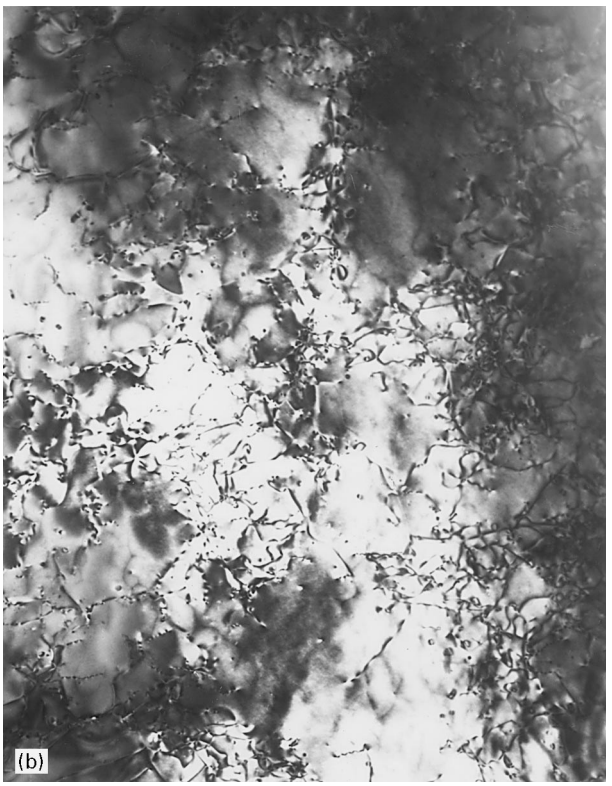

Figure 8 Transmission electron micrographs of the alloys deformed at a strain-rate of $1 \times 10^{-2}\ s^{-1}$ to a strain level of (a) 0.5 and (b) 1.25.

the as-received Al–13 wt % Si alloy taken at different strains up to failure. The figure also shows the association of grain-boundary cavities with silicon particles. The fracture surface shown in Fig. 7 also indicates the presence of particles at cavities at low strain-rates. At high strain-rates (i.e., 5×10^{-3}–$1 \times 10^{-2}\ s^{-1}$), the elongation to failure increases and failure is seen to occur by the formation of diffuse necks. Also, little or no cavitation is evident. At 557 °C, while the value of m is 0.17 at low to intermediate strain rates (i.e., 1×10^{-5}–$5 \times 10^{-4}\ s^{-1}$), m increases to 0.22 at $5 \times 10^{-3}\ s^{-1}$ (Fig. 2). This suggests that a combination of higher m values and low particle and grain coarsening is responsible for the high elongations observed at high strain rates. It has been previously suggested

[1] that at high strain rates, grain boundary sliding plays an important role in deformation. The transmission electron micrographs shown in Fig. 8 are suggestive of intense dislocation activity both within the grain and in the vicinity of the grain-boundary. It is thus felt that grain-boundary sliding is accommodated by dislocation motion not only within the grains but also in the vicinity of the grain-boundaries.

4. Discussion

Whilst several deformation mechanisms have been identified (Table I) as being operable at any given time, although over a range of temperature, stress and grain size, only one becomes rate-controlling [1, 2, 5–9]. Usually at temperatures below one-third of the absolute melting temperature, regardless of strain-rate, and grain-size, thermally-activated dislocations glide past obstacles and this process is the rate controlling one. The same mechanism is also probably rate controlling at higher temperature and high stresses i.e., $\sigma/G = 5 \times 10^{-3}$–$10^{-3}$ [2], where G is the temperature compensated shear modulus. At temperatures above half of the absolute melting temperature and σ/G values lower than 5×10^{-4}, dislocation creep mechanisms such as dislocation climb [10] or viscous glide [11] become rate controlling. When deformation is diffusion-controlled, the steady-state strain-rate $\dot{\varepsilon}$, is generally expressed by a dimensionless relation of the form [5]:

$$\frac{\dot{\varepsilon} kT}{DGb} = A\left(\frac{b}{d}\right)^{p}\left(\frac{\sigma}{G}\right)^{n} \cdots \quad (1)$$

where σ is the flow stress, A a substructure constant which is microstructure and mechanism related, b the Burger's vector, d the grain size, T the absolute temperature, p the grain size exponent, n the stress exponent, D the diffusion coefficient which is equal to $D_0 \exp(-Q/kT)$ where Q is the activation energy for diffusion and D_0 is the frequency factor, k the Boltzmann's constant and G is the temperature compensated shear modulus [12].

At a constant strain-rate this equation reduces to:

$$D = (\text{const.})\,\sigma^{-n} G^{n-1}|_{\dot{\varepsilon}, d} \cdots \quad (2)$$

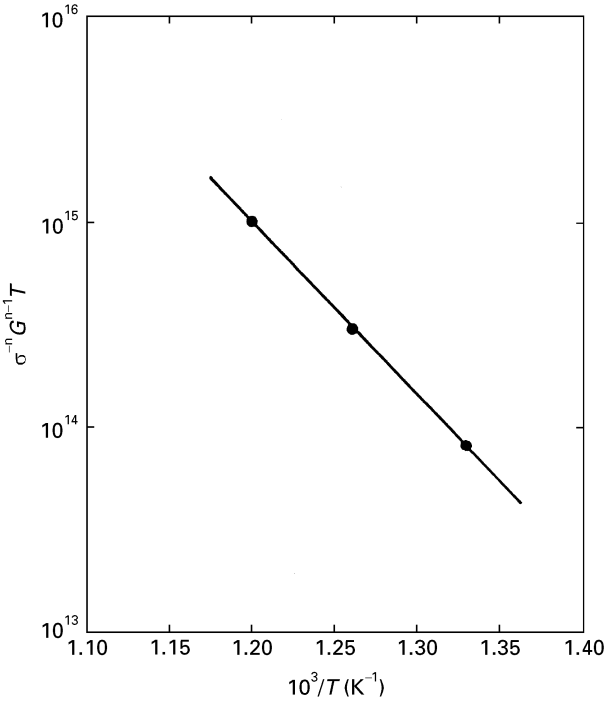

Figure 9 Activation energy plot for Al–13 wt % Si alloy: $\sigma^{-n}G^{-n-1}T$ versus $1/T$ at a strain rate ($\dot{\varepsilon}$) of $5 \times 10^{-4}\,s^{-1}$. From this plot Q can be calculated as 161.7 kJ mol^{-1}.

Since

$$D = D_0 \exp(-Q/RT) \cdots \quad (3)$$

It follows from Equations 1 and 3

$$Q = \frac{-R\delta \ln(\sigma^{-n} G^{n-1} T)}{\delta\left(\frac{1}{T}\right)} \cdots \quad (4)$$

and a semi-logarithmic plot of $\sigma^{-n} G^{n-1} T$ versus $1/T$ will yield a curve with the slope equal to $-Q/2.3\,R$. Such a plot is shown in Fig. 9 for Al–13 wt % Si at a strain-rate of $5 \times 10^{-4}\,s^{-1}$. The value of Q obtained from the slope in the figure is 161.7 kJ mol^{-1} which is close to the activation energy of 142 kJ mol^{-1} for volume diffusion in aluminium solid-solution [13]. In general, at high strain-rates fine-grained metals and

TABLE I Rate equations for various known deformation mechanisms

Mechanism	Rate equation	Reference
Thermally-activated glide of dislocations	$\dot{\varepsilon} = \varepsilon_0\left(\frac{\sigma}{G}\right)^{7/3} \exp\left\{-\frac{\Delta F}{kT}\left[0.5\,\sigma - y^{2/3}\left(\frac{\sigma}{G}\right)^{2/3}\right]\right\}$	[6]
Viscous glide of dislocations	$\dot{\varepsilon} = \left[\frac{0.35(kT)^2}{ce^2G^2b^2}\right]\frac{\tilde{D}Gb}{kT}\left(\frac{\sigma}{G}\right)^3$	[7]
Climb of dislocation	$\dot{\varepsilon} \simeq 2.5 \times 10^6 \frac{D_l Gb}{kT}\left(\frac{\sigma}{G}\right)^5$	[8]
Diffusional flow through lattice	$\dot{\varepsilon} \simeq 13 \frac{D_l Gb}{kT}\left(\frac{b}{d}\right)^2\left(\frac{\sigma}{G}\right)$	[8]
Diffusional flow along grain-boundaries	$\dot{\varepsilon} \approx \frac{150}{\pi}\frac{D_b Gb}{kT}\left(\frac{b}{d}\right)^3\left(\frac{\sigma}{G}\right)$	[8]
Superplastic flow	$\dot{\varepsilon} = \left[\frac{4\pi\omega}{hZ^2\tan\frac{\theta}{2}}\right]\frac{D_b Gb}{kT}\left(\frac{b}{d}\right)^2\left(\frac{\sigma}{G}\right)^2$	[9]

alloys deform by a dislocation climb creep mechanism [3]. From Fig. 2, the value of the stress sensitivity parameter, $n(=1/m)$ is close to 5 and hence at a strain-rate of $1\times10^{-2}\,s^{-1}$ and at a temperature of 557 °C, the climb of dislocations is believed to be the rate-controlling mechanism.

5. Conclusions

(1) The Al–13 wt % Si eutectic alloy with a grain-size of ~18 μm gives a maximum elongation of 250% at a strain-rate of $1\times10^{-2}\,s^{-1}$ and at a temperature of 557 °C.

(2) The maximum elongation is associated with a maximum value of 0.22 in contrast to an earlier investigation [1].

(3) The shapes of true stress–true strain curves are also different from those obtained in an earlier investigation, particularly at a strain rate of $4.6\times10^{-4}\,s^{-1}$ [1]. Strain softening behaviour, which is a manifestation of mechanical and microstructural effects, was observed in the present study as against a strain hardening and strain softening in the previous study, beyond maximum true stress.

(4) These differences are attributed to differences in processing routes of the alloy used by the two groups of investigators.

(5) Higher m-values, attributed to reduced particle- and grain-coarsening at strain-rates greater than $5\times10^{-3}\,s^{-1}$, are responsible for higher strains to failure.

(6) Since $n\sim5$ and the activation energy for high temperature flow is equal to that for volume diffusion at a strain-rate of $1\times10^{-2}\,s^{-1}$ the mechanism of high temperature flow is rate-controlled by the climb of dislocations over hard Si particles.

References

1. D. W. CHUNG and J. R. CAHOON, *Metal Science* **13** (1979) 635.
2. A. K. MUKHERJEE, in "Materials Science and Technology: A Comprehensive Treatment-Vol. 6", edited by R. W. Cahn, P. Haasen and E. J. Kramer (VCH Publishers Inc. New York, NY, 1993) p. 407.
3. B. P. KASHYAP and A. K. MUKHERJEE, *Res Mechanica* **17** (1986) 293.
4. E. E. UNDERWOOD, "Quantitative Stereology" (Addison-Wesley Press, New York, 1970) p. 149.
5. A. K. MUKHERJEE, J. E. BIRD and J. E. DORN, *Trans ASM* **62** (1969) 155.
6. A. ARIELI and A. K. MUKHERJEE, in "Creep and Fracture of Engineering Materials and Structures", edited by B. Wilshire and D. R. Owen (Pineridge Press, Swansea, 1981) p. 97.
7. J. WEERTMAN, *Trans Met. Soc. AIME* **28** (1960) 20.
8. J. E. BIRD, A. K. MUKHERJEE and J. E. DORN, in "Quantitative Relation Between Properties and Microstructure", edited by D. G. Brandon and A. Rosen (Univ. Press, Israel, 1969) p. 255.
9. A. ARIELI and A. K. MUKHERJEE, *Mat. Sci. and Engng.* **45** (1980) 61.
10. J. WEERTMAN, *Trans ASM* **61** (1968) 681.
11. *Idem*, *J. Appl. Phys.* **2B** (1957) 1185.
12. G. SIMMONS and H. WANG, "Single crystal elastic constant and calculated aggregated properties" (MIT Press, Cambridge, Massachusetts, 1971).
13. T. S. LUNDY and J. MURLOCK, *J. Appl. Phys.* **33** (1968) 1671.

Received 19 September 1994
and accepted 22 August 1995